Toxicology and Applied Pharmacology 412 (2021) 115387

Contents lists available at ScienceDirect

Toxicology and Applied Pharmacology

journal homepage: www.elsevier.com/locate/taap

Species-specific differences in the inhibition of 11β-hydroxysteroid dehydrogenase 2 by itraconazole and posaconazole

Silvia G. Inderbinen [a], Michael Zogg [a], Manuel Kley [a], Martin Smieško [b], Alex Odermatt [a,*]

[a] Swiss Centre for Applied Human Toxicology and Division of Molecular and Systems Toxicology, Department of Pharmaceutical Sciences, University of Basel, Klingelbergstrasse 50, Basel 4056, Switzerland
[b] Computational Pharmacy, Department of Pharmaceutical Sciences, University of Basel, Klingelbergstrasse 61, Basel 4056, Switzerland

ARTICLE INFO

Keywords:
Glucocorticoid
Pseudohyperaldosteronism
Hypertension
11beta-Hydroxysteroid Dehydrogenase
Azole Fungicide
Species Difference

ABSTRACT

11β-hydroxysteroid dehydrogenase 2 (11β-HSD2) converts active 11β-hydroxyglucocorticoids to their inactive 11-keto forms, thereby preventing inappropriate mineralocorticoid receptor activation by glucocorticoids. Disruption of 11β-HSD2 activity by genetic defects or inhibitors causes the syndrome of apparent mineralocorticoid excess (AME), characterized by hypokalemia, hypernatremia and hypertension. Recently, the azole antifungals itraconazole and posaconazole were identified to potently inhibit human 11β-HSD2, and several case studies described patients with acquired AME. To begin to understand why this adverse drug effect was missed during preclinical investigations, the inhibitory potential of itraconazole, its main metabolite hydroxyitraconazole (OHI) and posaconazole against 11β-HSD2 from human and three commonly used experimental animals was assessed. Whilst human 11β-HSD2 was potently inhibited by all three compounds (IC_{50} values in the nanomolar range), the rat enzyme was moderately inhibited (1.5- to 6-fold higher IC_{50} values compared to human), and mouse and zebrafish 11β-HSD2 were very weakly inhibited (IC_{50} values above 7 μM). Sequence alignment and application of newly generated homology models for human and mouse 11β-HSD2 revealed significant differences in the C-terminal region and the substrate binding pocket. Exchange of the C-terminus and substitution of residues Leu170,Ile172 in mouse 11β-HSD2 by the corresponding residues His170,Glu172 of the human enzyme resulted in a gain of sensitivity to itraconazole and posaconazole, resembling human 11β-HSD2. The results provide an explanation for the observed species-specific 11β-HSD2 inhibition by the studied azole antifungals. The obtained structure-activity relationship information should facilitate future assessments of 11β-HSD2 inhibitors and aid choosing adequate animal models for efficacy and safety studies.

1. Introduction

11β-hydroxysteroid dehydrogenase type 2 (11β-HSD2) catalyzes the oxidation of potent 11β-hydroxyglucocorticoids (cortisol in human and fish, corticosterone in rodents) to inactive 11-ketoglucocorticoids (cortisone in human and fish, 11-dehydrocorticosterone in rodents). In mineralocorticoid target tissues such as kidney, colon, salivary and sweat glands, 11β-HSD2 has a gate-keeper function to regulate the access of cortisol to mineralocorticoid receptors (MR), thereby allowing specificity of aldosterone to activate MR (Edwards et al. 1988; Funder et al. 1988; Odermatt and Kratschmar 2012). By this mechanism, 11β-HSD2 has an important role in the regulation of the electrolyte balance. Loss of function mutations in the gene encoding 11β-HSD2 lead to the syndrome of apparent mineralocorticoid excess (AME), caused by excessive MR activation by cortisol (Mune et al. 1995; Wilson et al. 1995; White et al. 1997). These patients suffer from pseudohyperaldosteronism with hypokalemia, hypernatremia, water retention and hypertension, with typically low renin and aldosterone levels along with increased plasma and urinary cortisol to cortisone ratios. Acquired forms of AME can be caused by the excessive consumption of licorice, containing the potent 11β-HSD inhibitor glycyrrhetinic acid (GA) (reviewed in (Ferrari 2010)), and, as more recently reported, by the systemically administered azole antifungals posaconazole and itraconazole (Thompson et al., 2017; Barton et al. 2018; Boughton et al. 2018;

Abbreviations: 11β-HSD2, 11β-hydroxysteroid dehydrogenase type 2; AME, Apparent mineralocorticoid excess; C-terminal, Carboxy-terminal; GA, Glycyrrhetinic acid; MR, Mineralocorticoid receptors; OHI, Hydroxyitraconazole; WT, Wild type.

* Corresponding author.
E-mail address: Alex.Odermatt@unibas.ch (A. Odermatt).

https://doi.org/10.1016/j.taap.2020.115387
Received 22 October 2020; Received in revised form 11 December 2020; Accepted 23 December 2020
Available online 31 December 2020

Hoffmann et al. 2018; Wassermann et al. 2018; Thompson et al., 2019).

11β-HSD2 is also highly expressed in the placenta, where it exerts a barrier function to protect the developing fetus from high maternal cortisol concentrations (Albiston et al. 1994; Stewart et al. 1995). Inhibition of placental 11β-HSD2 is associated with intra-uterine growth restriction and results in an increased risk for cardio-metabolic diseases in later life of the off-spring (Edwards et al. 1993; Lindsay et al. 1996; Seckl et al. 2000; Odermatt 2004). Given its important physiological functions, it is crucial to identify exogenous substances inhibiting 11β-HSD2 that might cause adverse health effects in human. Furthermore, 11β-HSD2 was recently found to be involved in oxysterol metabolism, with possible roles in the regulation of the immune system and in the control of cancer cell properties (Voisin et al. 2017; Raleigh et al. 2018; Beck et al. 2019a; Beck et al. 2019b). However, whether a disturbance of these functions contributes to the observed adverse health effects upon inhibition of 11β-HSD2 remains unknown.

Animal models are widely applied for efficacy and safety studies during the development and testing of novel drugs. However, the fact that the itraconazole- and posaconazole-induced pseudohyperaldosteronism remained undetected in preclinical investigations emphasizes the importance to understand species-specific differences as well as caution when trying to extrapolate findings from animal studies to human. The most frequently used animal species for preclinical toxicological studies is the rat, whereas the mouse is most widely used for mechanistic investigations, including transgenic lines. Additionally, the importance of zebrafish has gained considerable attraction due to the low cost and because experiments with larvae during the first 96 h are not considered as animal experiment (Planchart et al. 2016; Wrighton et al. 2019).

Rather few studies addressed species-specific differences in 11β-HSD2 so far. Nevertheless, *in vitro* studies showed potent inhibitory effects of the anabolic androgenic steroid fluoxymesterone (Fürstenberger et al. 2012) and of dithiocarbamates (Meyer et al. 2012) against human but not rodent or zebrafish 11β-HSD2, respectively. Furthermore, itraconazole and posaconazole were shown to be potent inhibitors of recombinant human 11β-HSD2 in *in vitro* experiments (Beck et al. 2017), whereas measurements performed in whole rat an mouse kidney homogenates suggested much weaker inhibitory effects in these species. However, in whole renal homogenates the compounds could have been metabolized and therefore no longer able to inhibit 11β-HSD2 activity, thus requiring a direct comparison of inhibitory effects on recombinant enzymes determined in the same cellular background. Nevertheless, no significant adverse effects were observed after inspection of endocrine parameters in preclinical rat studies following exposure to itraconazole (Van Cauteren et al. 1987). This suggests that due to species-differences rodents may not serve as suitable surrogate models to study effects on 11β-HSD2 in human.

The present study aimed to compare inhibitory potencies of posaconazole, itraconazole and its main metabolite hydroxyitraconazole (OHI) towards recombinant human, rat, mouse and zebrafish 11β-HSD2. A more detailed comparison then focused on the human and mouse enzyme. For this purpose, new homology models, molecular docking calculations as well as site-directed mutagenesis and enzyme activity assays with chimeric proteins were applied to elucidate the structure-function relationships of the species-specific differences in the mechanism of inhibition by the azole antifungals.

2. Material and methods

2.1. Chemicals and reagents

[1,2,6,7-^{3}H]-cortisol was obtained from Perkin-Elmer (Boston, MA, USA) and hydroxyitraconazole (OHI) from Carbosynth (Berkshire, UK). All other chemicals were from Sigma-Aldrich (Buchs, Switzerland) if not stated otherwise.

2.2. Cell culture

Human embryonic kidney-293 cells (HEK-293) were purchased from ATCC (Manassas, VA, USA). Cells were cultured in Dulbecco's modified Eagle medium (DMEM) supplemented with 4.5 g/L glucose, 10% fetal bovine serum (S1810-500, Biowest, Nuaillé, France), 100 U/mL penicillin, 0.1 mg/mL streptomycin, 10 mM HEPES buffer (pH 7.4) and 1% MEM non-essential amino acids (Bio Concept, Allschwil, Switzerland) at standard conditions (37 °C and humidified 5% CO_2).

2.3. Molecular cloning

All chimeric proteins were designed to bear a C-terminal Flag-tag (DYKDDDDK) and were cloned into the pcDNA3.1 vector (Invitrogen, Carlsbad, CA, USA) (schematic overview of the chimera in Fig. 3). The chimera A (human 11β-HSD2 with mouse C-terminus), B (mouse 11β-HSD2 with human C-terminus), C (human 11β-HSD2 with mouse cassette) and D (mouse 11β-HSD2 with human cassette) were generated by a sequence overlap extension approach based on the human (Odermatt et al. 1999) or mouse 11β-HSD2 cDNA (NM_008289.2 in pcDNA3.1 from GenScript, Piscataway Township, NJ, USA). The fragments were amplified with complementary overhangs of the cassette corresponding to residues 268–277 for human (5'-GAGTCAGTGA-GAAACGTGGGTCAGTGGGAA-3′) and mouse 11β-HSD2 (5'-GATG-CAGTGACTAATGTGAACCTCTGGGAG-3′) (oligonucleotide primers used for amplification are shown in Suppl. Table 1). The two purified fragments containing the complementary overhangs were supplied in an equimolar ratio, followed by a PCR reaction using primers at the 5′ and 3′ end of the entire sequence for amplification. PCR reactions were carried out using iProof™ High-Fidelity DNA polymerase (Bio-rad, Hercules, CA, USA). The final PCR product was digested with Hind-III HF and Kpn-I HF (New England Biolabs, NEB, Ipswich, MA, USA) and ligated into pcDNA3 by T4 ligase (NEB).

Chimera E (human 11β-HSD2 with His170Leu,Glu172Ile) and G (chimera A with His170Leu,Glu172Ile) were obtained by site directed mutagenesis using Pfu polymerase (NEB) and TaKaRa PrimeSTAR GXL polymerase (Takara Bio Inc., Kusatsu, Japan). Oligonucleotide primers were designed to achieve a circular nicked PCR-product. Template DNA was removed by a *Dpn* I digest (NEB), and the PCR product was transformed into competent bacterial cells for amplification. Chimera F (mouse 11β-HSD2 bearing mutations Leu170His,Ile172Glu) and H (chimera B with mutations Leu170His,Ile172Glu) were generated utilizing iProof ™ High-Fidelity DNA polymerase, resulting in a linear unphosphorylated PCR-product. To facilitate re-circularization, the 5′-ends were phosphorylated by T4 polynucleotide kinase (NEB) prior to ligation by T4 ligase. After Dpn I digest, the clones were transformed into competent bacterial cells. Sequences were verified by Sanger sequencing (Microsynth, Balgach, Switzerland).

2.4. Determination of the inhibition of wild type and mutant 11β-HSD2 activity by azole antifungals

HEK-293 cells (2×10^6 cells per 10 cm cell culture dish) were incubated for 24 h and transiently transfected with plasmids encoding mouse (NM_008289.2), rat (NM_017081.2) or zebrafish 11β-HSD2 (NM_212720.2), or with chimera A-H, using the calcium precipitation method. All constructs were C-terminally flag epitope tagged and cloned into pcDNA3. At 48 h post-transfection, the cells were washed with PBS, collected in 2 mL ice-cold PBS per 10 cm dish, aliquoted (200 μL or 400 μL) and centrifuged at 4 °C for 4 min at 16,000 × *g*. Subsequently, supernatants were discarded, pellets shock-frozen and stored at −80 °C. For the analysis of human 11β-HSD2 activity, HEK-293 cells stably expressing 11β-HSD2 (AT8 clone) were utilized as described earlier (Inderbinen et al., 2020). Cell pellets were suspended in 400 μL TS2 buffer (NaCl 100 mM, EGTA 1 mM, EDTA 1 mM, $MgCl_2$ 1 mM, sucrose 250 mM, Tris-HCl 20 mM, pH 7.4) and lysed by sonication (UP50H

sonicator, Hielscher Ultrasonics). Conditions for each batch of cell pellets were optimized to reach 20–30% substrate to product conversion rate. Lysates were incubated with test substances or vehicle control (DMSO), 50 nM cortisol (containing 10 nCi of [1,2,6,7-^{3}H] cortisol) and 500 μM NAD^+ in a total volume of 22 μL TS2 buffer at 37 °C. The DMSO concentration was kept below 1.2%. At this concentration the solvent did not affect enzyme activity. After 10 min (human, chimera B) or 20 min (mouse, rat, zebrafish, chimera A, C, D, E, F and H), reactions were stopped by adding excess amounts of unlabeled cortisone and cortisol in methanol (1:1, 2 mM each). Samples were separated by thin-layer chromatography (mobile phase chloroform/methanol; 9:1), dissolved in scintillation cocktail (IRGASAFE Plus, Zinsser Analytic, Frankfurt am Main, Germany) and radioactivity was measured by liquid scintillation counting (Packard, Connecticut, USA). Experiments were repeated at least three times independently and data were normalized to vehicle control.

2.5. Homology model and docking

As there is no crystal structure of 11β-HSD2 available to date, the modeling study aiming at explaining the mechanism of inhibition of the human and mouse enzyme variants was initiated with homology modeling using the SwissModel homology modeling platform (https://swissmodel.expasy.org). The primary FASTA sequence of human 11β-HSD2 was used as input to the SwissModel web-server. Up to thirty homology models were built based on templates identified by sequence similarity to existing proteins.

Eight homology models were built using template structures of 17β-HSD1 (various PDB IDs), twenty models were based on the template structure of 11β-HSD1 (various PDB IDs), one model on the template structure of 3-oxoacyl-[acyl-carrier-protein] reductase (PDB ID: 3u9l) and finally one on the template structure of a putative short chain dehydrogenase (PDB ID: 5u4s).

Visual inspection of eight models based on template structures of 17β-HSD1 yielded no satisfactory model with respect to the placement of both the substrate and cofactor NAD^+ and the dehydrogenation reaction that the enzyme is supposed to catalyze (at position 11). The assumed pose of the cofactor within the active site was found to interfere with backbone elements of the built homology models, rendering them unsuitable for further processing. This is in contrast with a previous study that, however, used a complex multi-step refinement and optimization procedure to obtain a valid putative model (Yau et al. 2017).

Therefore, we focused on twenty homology models based on the template structure of 11β-HSD1, *i.e.* the closest relative in this enzyme family. Their Global Model Quality Estimation (GMQE) scores did not differ substantially from those of the 17β-HSD1 based models (0.40 *vs* 0.44 for the best scored models). Both cofactor (NAD^+) and substrate (cortisol) poses were reconstructed by a rigid body transfer and subsequent structure modification from the 11β-HSD1 structure with the PDB ID 1y5r (cofactor, NADPH; ligand, corticosterone) after protein alignment. Most of the 11β-HSD-based models did not show any unfavorable steric backbone clashes with the assumed cofactor pose and allowed placing of the natural substrate into the active site. In analogy to human 11β-HSD2 models, we built thirty homology models using the mouse FASTA sequence. For both species, homology models based on guinea pig 11β-HSD1 (PDB ID: 3g49) revealed the most reliable models that were utilized for further investigations.

The structure-activity relationships-conform binding modes of the natural substrate cortisol at both human and mouse homology models were found by manual docking. As mentioned earlier, the corticosterone pose relative to the nicotinamide moiety of NAD^+ and key catalytic residues Tyr232 and Ser219, as it occurs in homologous 11β-HSD1 structure with PBD ID 1y5r, was used as a reference starting point. The 17α-hydroxy group was added, turning corticosterone to cortisol, and together with the hydroxymethylcarbonyl group at position 17β oriented for the most optimal interaction with the nearby backbone, cofactor and side-chain (in this order of preference) H-bond donors and acceptors. As the C-terminal part of 11β-HSD2 interacting with azole fungicides could not be sufficiently resolved in homology modeling, only the 1-(butan-2-yl)-4-phenyl-4,5-dihydro-1H-1,2,4-triazol-5-one part of itraconazole responsible for the sensitivity towards 11β-HSD2 was manually docked. The binding mode was constructed by satisfying the carbonyl H-bond acceptor with a properly directional hydrogen bond donor from Tyr232 while paying attention to minimizing the steric clashes with the other residues in the active site. The manual docking was performed in Maestro modeling environment (Maestro, version 10.4, Schrödinger, LLC, New York, NY, 2015). Protein Preparation Wizard minimizer routine with OPLS_2005 force field was used to relax manually constructed protein-ligand complexes and Maestro was used for visualization (Sastry et al. 2013).

2.6. Statistical analysis

Data were analyzed using two-way ANOVA with Bonferroni's *post hoc* tests in the GraphPad Prism 5 software. Values represent mean ± SD.

3. Results

3.1. Species-specific differences in the inhibition of 11β-HSD2 by posaconazole, itraconazole and OHI

The posaconazole-, itraconazole- and OHI-dependent inhibition of cortisol oxidation by 11β-HSD2 from the four different species human, mouse, rat and zebrafish was determined in lysates of HEK-293 cells expressing recombinant enzyme (Fig. 1, Table 1). Itraconazole, OHI and posaconazole potently inhibited the human enzyme, with IC_{50} values of 121 ± 30, 187 ± 56 and 512 ± 79 nM, respectively. Itraconazole and OHI were approximately 6-fold less active towards the rat enzyme, whereas posaconazole was only 1.6-fold less active. In contrast, all three azole antifungals showed only very weak inhibitory effects towards mouse and zebrafish 11β-HSD2, with IC_{50} values above 7 μM.

3.2. Comparison of human, mouse, rat and zebrafish 11β-HSD2 protein sequences

To begin to understand which regions of the sequence are responsible for the observed species-specific differences in 11β-HSD2 inhibition by the azole antifungals, the protein sequences of human, mouse, rat and zebrafish 11β-HSD2 were aligned (Fig. 2). The justbio (justbio.com) alignment tool was utilized to analyze protein sequences (human: NP_000187.3; mouse: NP_032315.2; rat: NP_058777.1; zebrafish: NP_997885). The catalytic triad Ser219, Tyr232 and Lys236, the cofactor-binding site in the Rossmann-fold (Gly89-X-X-X-Gly93-X-Gly95) and most of the α-helices and β-sheets are conserved among the four species. As expected, human 11β-HSD2 shares higher sequence similarities with mouse and rat enzymes than with that of the zebrafish. Significant differences were detected in the C-terminal regions. The mouse enzyme is 19 amino acids shorter than its human counterpart, while the rat C-terminus is more similar to that of the human enzyme. Thus, we hypothesized that the variable C-terminal region could be responsible for the differences in the inhibition of human and mouse 11β-HSD2 by the investigated azole fungicides. Previous predictions using rigid homology models of the human and mouse enzyme suggested a different orientation of Trp276 that would cause steric hindrance in the mouse enzyme and prevent binding of posaconazole, itraconazole and OHI (Beck et al. 2017). Additionally, Arg279 was proposed to stabilize the binding of itraconazole and OHI in the human enzyme but not in mouse 11β-HSD2, where this residue did not seem to form interactions with the investigated azole fungicides (Beck et al. 2017; Beck et al. 2020a). Interestingly, Trp276 and Arg279 are both conserved in human and mouse 11β-HSD2. Nevertheless, a closer inspection of the sequence upstream of these two amino acids led to the

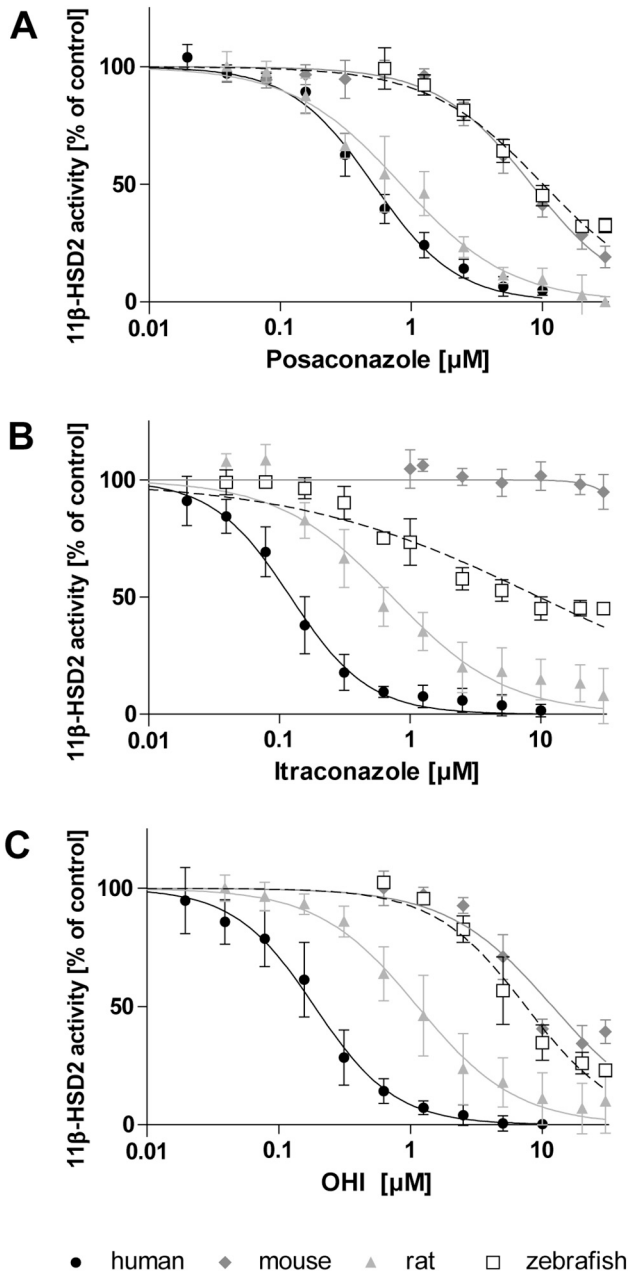

Fig. 1. Inhibition of human, mouse, rat and zebrafish 11β-HSD2 activity. Lysates of HEK-293 cells expressing recombinant 11β-HSD2 of the respective species were incubated for 10 min (human) or 20 min (mouse, rat, zebrafish) in the presence of 50 nM cortisol, 500 μM NAD^+ and increasing concentrations of posaconazole (A), itraconazole (B) or OHI (C). Substrate conversion was normalized to that of the vehicle control (DMSO; 0.3% for posaconazole, 0.6% for itraconazole and 1.2% for OHI). Inhibition curves were fitted and analyzed by non-linear regression. Data shown are from at least three independent experiments and represent mean ± SD.

hypothesis that the rather bulky amino acids Arg271 and Gln275 in human compared to Thr271 and Leu275 in mouse 11β-HSD2 might result in a different orientation of Trp276 and Arg279 in the two species. Thus, in a next step, the species difference between human and mouse 11β-HSD2 was investigated by site-directed mutagenesis and generation of chimeric proteins.

Table 1
IC_{50} values for human, mouse, rat and zebrafish 11β-HSD2 of posaconazole, itraconazole and OHI. 11β-HSD2 activity was determined in lysates of HEK-293 cells expressing the recombinant enzyme of the respective species. The conversion of cortisol to cortisone was measured in the presence of increasing concentrations of inhibitor. Inhibition curves were fitted and analyzed by non-linear regression. Data were normalized to vehicle control and represent mean ± SD of at least three independent experiments. * % remaining activity at the highest concentration of 30 μM.

	Inhibition of 11β-HSD2 activity: IC_{50} [μM]			
	Human	Mouse	Rat	Zebrafish
Posaconazole	0.512 ± 0.079	8.21 ± 0.56	0.835 ± 0.142	10.1 ± 0.5
Itraconazole	0.121 ± 0.030	(95%)*	0.729 ± 0.592	9.80 ± 1.96
OHI	0.187 ± 0.056	11.9 ± 2.5	1.13 ± 0.96	7.48 ± 1.68

3.3. The role of the C-terminal region and of residues 268–277 on the inhibition of human and mouse 11β-HSD2 by azole fungicides

Four different chimera were constructed to investigate the role of the C-terminus in the different response of human and mouse 11β-HSD2 to the azole antifungals (Fig. 3A). Chimera A contains the sequence of human 11β-HSD2 up to residue 268, followed by the mouse C-terminus. Chimera B represents the complementary construct with the mouse sequence up to position 268, followed by the human C-terminus. To investigate the impact of the amino acids 268–277 on the orientation of Trp276 and Arg279, this cassette of 8 amino acids was exchanged between human and mouse, resulting in chimera C (human enzyme with the mouse cassette) and D (mouse enzyme with the human cassette). These chimeric proteins were expressed similar to the wild type enzymes and able to convert cortisol to cortisone (Suppl. Fig. 1).

We hypothesized that chimera A and C would show a loss of inhibition by the azole fungicides compared to human 11β-HSD2 and that chimera B and D would show a gain of inhibitory effect compared to the mouse enzyme. Therefore, lysates of HEK-293 cells expressing the respective protein were subjected to enzyme activity assays in the absence and presence of 1 μM or 10 μM of the indicated azole fungicide (Fig. 4). Substitution of the human C-terminal region by that of the mouse enzyme in chimera A significantly decreased the inhibitory effect of the tested azole fungicides (Fig. 4). The analogous substitution, *i.e.* mouse enzyme bearing the human C-terminal region (chimera B), resulted in a trend to increased sensitivity towards itraconazole but not towards posaconazole or OHI (Figure 4Fig. 4). Substitution of the human sequence upstream of Trp276 by the corresponding mouse cassette (chimera C) as well as the analogous exchange in the mouse enzyme (chimera D) did not affect the azole fungicide-mediated inhibition (data not shown).

3.4. Use of homology models to study differences between human and mouse 11β-HSD2

Due to the limitations of previously used rigid homology models, more flexible models of human and mouse 11β-HSD2 were developed to study further species-specific differences. The new models both predicted comparable hydrogen bonds between Ser219 and Tyr232 with the C11-hydroxyl on cortisol and the cofactor, essential for catalytic activity (Fig. 5, Video 1 and Video 2). Additionally, Tyr226 forms a hydrogen bond with the C3-carbonyl on cortisol, and the C21-hydroxyl on cortisol forms a hydrogen bond with NAD^+ in both species. Predicted differences include hydrogen bonds between Gln342 and the C3-carbonyl on cortisol as well as between NAD^+ and Ser269 in human 11β-HSD2 that are both absent in the mouse enzyme. Furthermore, Ser269 forms a hydrogen bond with the C17-hydroxyl on cortisol, while the mouse enzyme has an alanine at this position. Notably, the new models predicted differences in the orientation and interactions of the loop consisting of residues 168–180 that are lining the active site. A

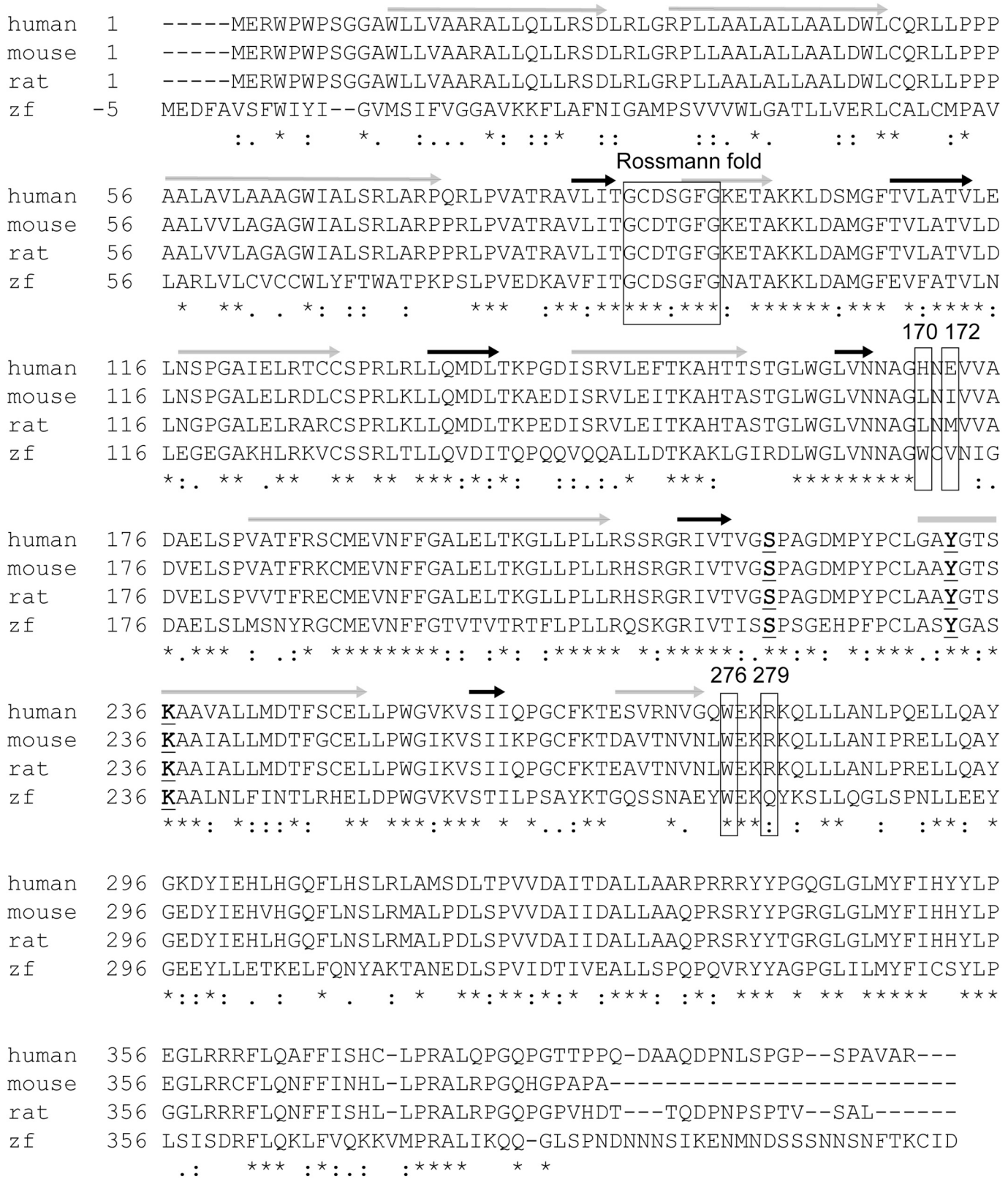

Fig. 2. Alignment of human, mouse, rat and zebrafish 11β-HSD2 protein sequences. Symbols are coded as followed: grey arrow, α-helix; black arrow, β-sheets; rectangles, cofactor-binding site in the Rossmann-fold, and positions 170, 172, 276 and 279; underlined and bold letter, active site; (*), fully conserved residues; (:), residues with considerably similar properties; (.), residues with moderately similar properties.

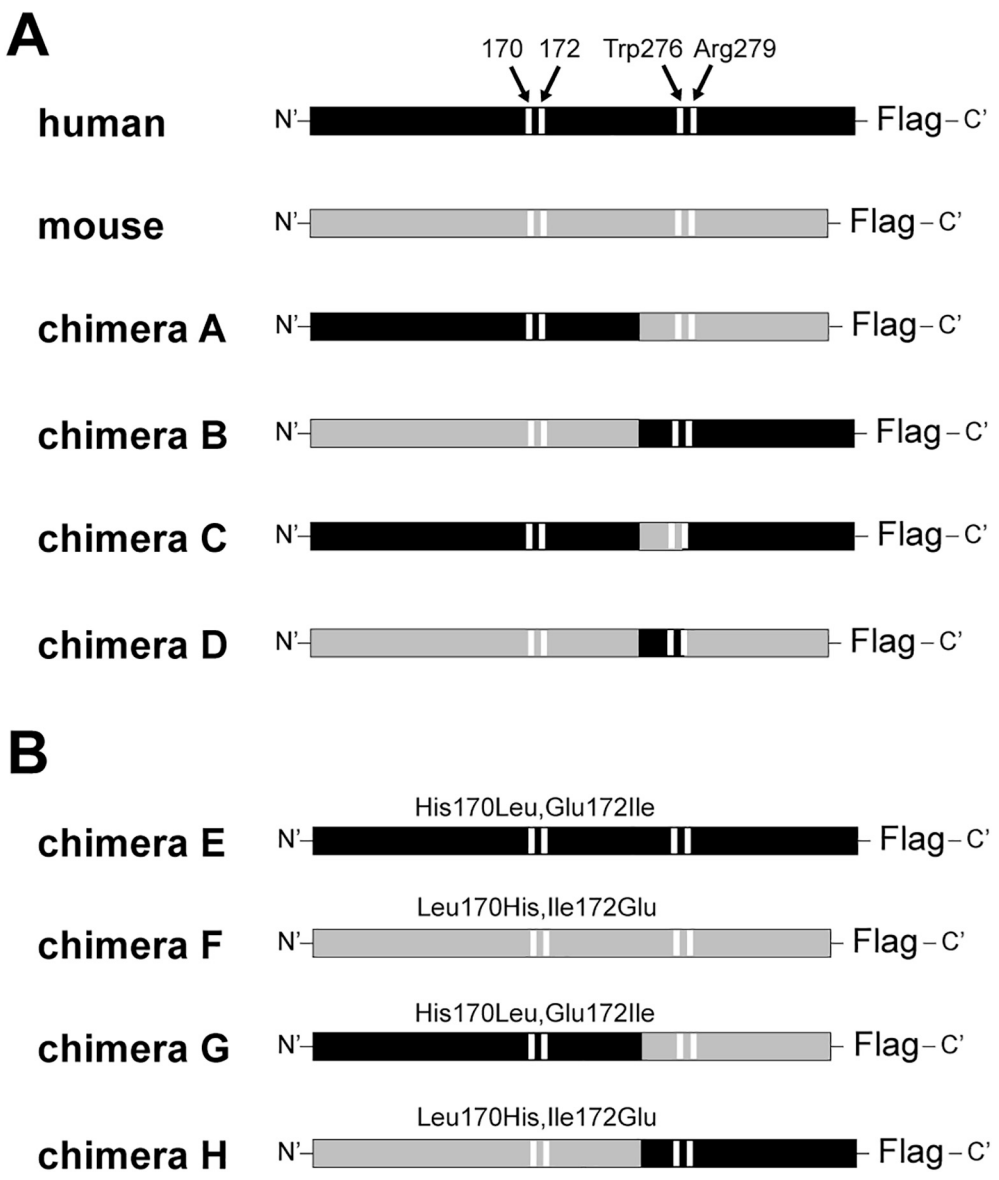

Fig. 3. Schematic representation of the cloned 11β-HSD2 mutants. Human sequence is indicated in black, mouse sequence in grey and the positions 170, 172, 276 and 279 are represented by white bars. All sequences were cloned into pcDNA3 and carry a C-terminal FLAG-tag.

closer look in human 11β-HSD2 on the binding site region in the vicinity of the steroid substrate D-ring, dictating selectivity to cortisol, indicated that the loop portion around histidine residue 170 (His170) could be responsible for interspecies differences in the enzyme selectivity. Optimization of a human homology model built on the guinea pig 11β-HSD1 (PDB ID: 3g49) template showed that His170 offers an ideal hydrogen bonding interaction to the cortisol C20 carbonyl (Fig. 5A, Video 1). Due to the particular pKa properties of His170, it may also provide positive charge for compensating the negative charge of the cofactor's phosphate groups. Furthermore, the human 11β-HSD2 model bears a charged glutamic acid at position 172 (Glu172) in close proximity to His170. Even though Glu172 is not directly involved in substrate binding, it may influence the structure of the protein considerably due to its charge and positioning preference towards the solvent. Interestingly, Glu172 was proposed earlier to interact with Leu179 and disruption of the stabilization of a flexible turn in the AME causing mutant Leu179Arg may contribute to the observed loss of function (Yau et al. 2017).

In contrast, the active site loop (residues 168–180) of mouse 11β-HSD2 contains more lipophilic residues (Leu170, Ile172) compared to the human structure (Fig. 5B, Video 2). These two lipophilic residues were predicted to hide from the solvent into the interior of the active site cavity, causing substantial reshaping of the backbone path in the area critical for substrate binding and slightly limiting the accessibility of the pocket. This still allowed binding of endogenous substances like cortisol, but bulky compounds like itraconazole, OHI and posaconazole (Suppl. Fig. 2) may experience less favorable interactions in the mouse compared to the human enzyme. For the reasons described above, we aimed to investigate to which extent the residues at position 170 and 172 are involved in the observed species-dependent 11β-HSD2 inhibition by the studied azole antifungals.

3.5. Effect of residues at positions 170 and 172 on the inhibition of human and mouse 11β-HSD2 by azole fungicides

To test the relevance of the residues at positions 170 and 172 for the azole fungicide-dependent inhibition of human 11β-HSD2, His170 and Glu172 were mutated to the respective residues in mouse 11β-HSD2 (Leu170, Ile172) in human wild type 11β-HSD2 (chimera E) or in the human enzyme bearing the mouse C-terminal region (chimera G) (Fig. 3B). The analogous exchange in mouse wild type (chimera F) and

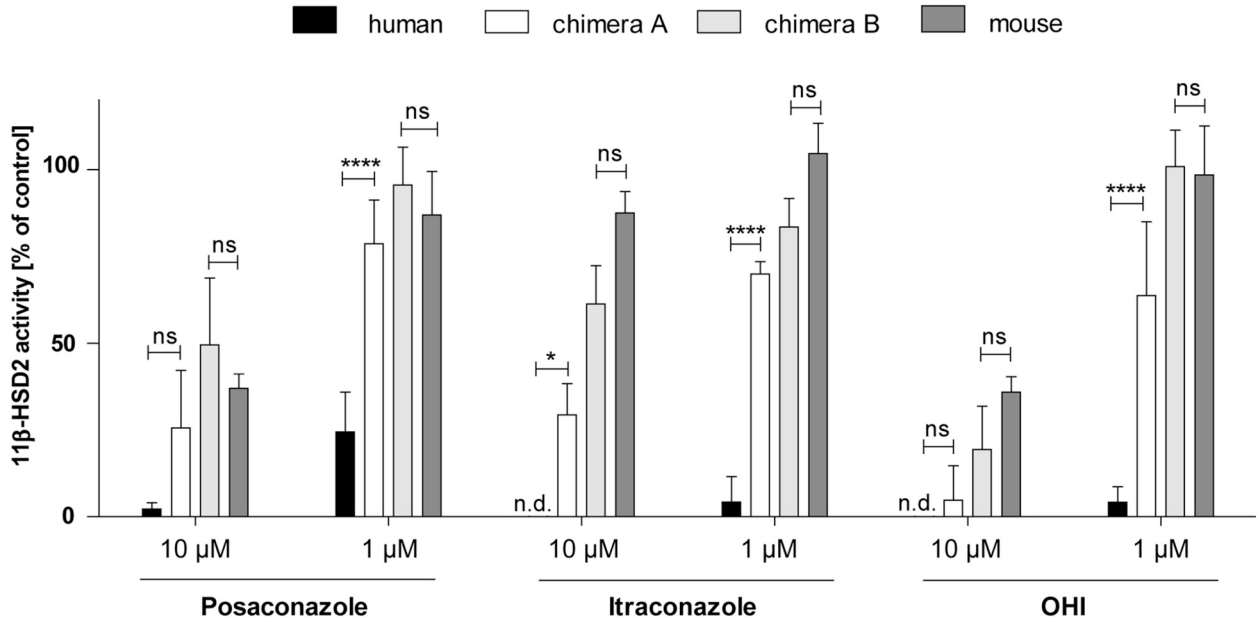

Fig. 4. Effect of the substitution of the C-terminal region of human and mouse 11β-HSD2 on azole fungicide-mediated inhibition. Lysates of HEK-293 cells expressing the indicated 11β-HSD2 construct were incubated for 10 min (human, chimera B) or 20 min (mouse, chimera A) with 50 nM cortisol, 500 μM NAD^+ and 1 μM or 10 μM of test substances. Substrate conversion was normalized to vehicle control (0.4% DMSO). Data from three independent experiments represent mean ± SD. Two-way ANOVA with Bonferroni's *post hoc* test, *p* values: * < 0.05, **** < 0.0001 and ns (not significant), n.d. (not detected).

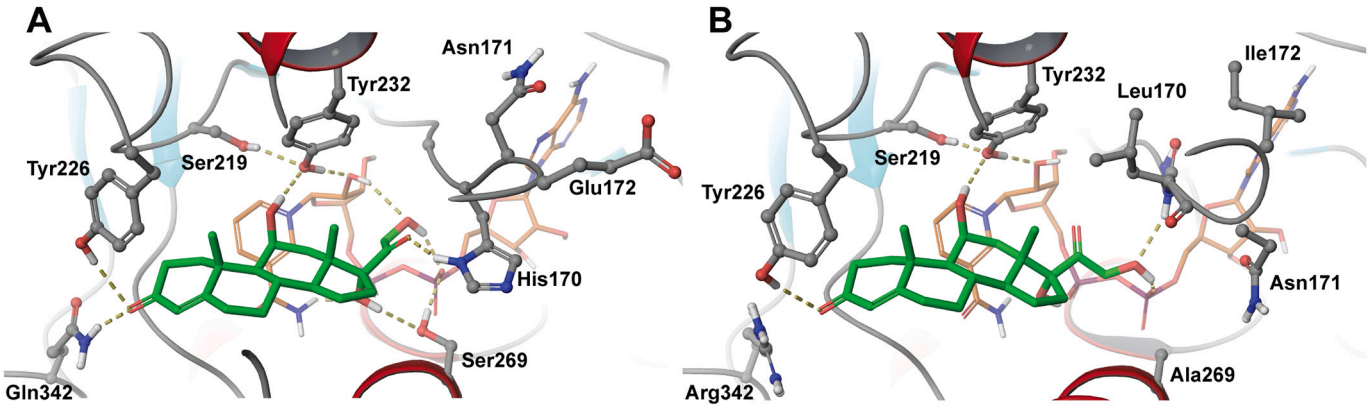

Fig. 5. Predicted binding of cortisol (green) and NAD^+ (orange) to 11β-HSD2. A) human and B) mouse 11β-HSD2 homology models. Dashed yellow lines indicate relevant hydrogen bond interactions (fulfilling directionality and distance criteria <2.8 Å) for protein-ligand binding. (For interpretation of the references to colour in this figure legend, the reader is referred to the web version of this article.)

mouse 11β-HSD2 bearing the human C-terminus (chimera H) were constructed as well. The chimeric enzymes were well expressed and active in intact HEK-293 cells, except of chimera G that seemed to be unstable as indicated by its reduced expression following detection by western blot and based on the loss of enzyme activity in assays using lysates of HEK-293 cells transiently expressing chimera G (Supp. Fig. 1).

Human 11β-HSD2 with the substitution His170Leu,Glu172Ile (chimera E) displayed significantly decreased inhibition by the three azole fungicides tested at 1 μM (Fig. 6). The analogous mutation Leu170His,Ile172Glu in the murine enzyme (chimera F) significantly increased and tended to increase the sensitivity towards itraconazole and OHI, respectively. In contrast, chimera F and mouse 11β-HSD2 were similarly inhibited by posaconazole. Importantly, replacing the C-terminal region in the mouse sequence by that from human and introducing substitutions Leu170His,Ile172Glu (chimera H) changed the inhibition pattern for the three azole antifungals almost to that of the human enzyme (Fig. 6). Unfortunately, the combination of replacing the C-terminus of the human enzyme by that of the mouse and introducing substitutions His170Leu,Glu172Ile (chimera G), was not stable and could thus not be tested.

Next, concentration-dependence curves were determined for the most potent 11β-HSD2 inhibitor, itraconazole (Fig. 7). Whilst an IC_{50} of itraconazole for human 11β-HSD2 of 121 ± 30 nM was obtained, a more than 15-fold weaker inhibition (2.17 ± 1.66 μM) was determined for chimera E carrying the His170Leu,Glu172Ile substitution (Table 2). Exchange of the human C-terminus by that of the mouse (chimera A) decreased the inhibitory potency of itraconazole by a factor of 30 (IC_{50} value of 3.55 ± 1.81 μM). The combination of C-terminus exchange and His170Leu,Glu172Ile substitution could not be assessed due to the instability of chimera G. The murine enzyme showed a residual activity of about 95% at the highest itraconazole concentration tested (30 μM) and an IC_{50} value could not be determined. Regarding mouse 11β-HSD2, a gain of sensitivity towards inhibitory effect of itraconazole could be observed by replacing the C-terminal region by that from human (chimera B, 58% residual enzyme activity at 30 μM) or by introducing the substitution Leu170His,Ile172Glu (chimera F) (IC_{50} value of 6.34 ±

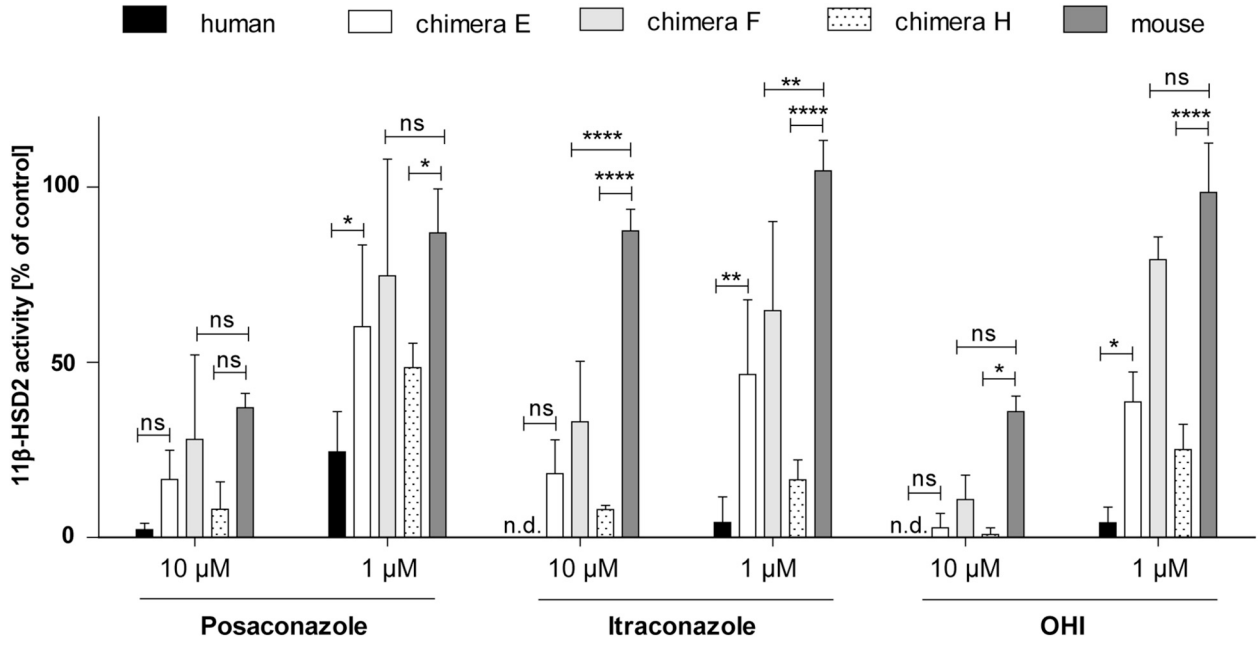

Fig. 6. Comparison of the posaconazole-, itraconazole- and OHI-dependent inhibition of human and mouse 11β-HSD2 with that of chimera E, F and H. Lysates of HEK-293 cells expressing recombinant 11β-HSD2 of the indicated species or the respective chimera were incubated for 10 min (human) or 20 min (mouse, chimeras) with 50 nM cortisol, 500 μM NAD^+ and 1 μM or 10 μM of the test compounds. Substrate conversion was normalized to that of the vehicle control (0.4% DMSO). Data represent mean ± SD from three independent experiments. Data were analyzed by two-way ANOVA with Bonferroni's *post hoc* test. *P* values: * < 0.05, ** < 0.01, **** < 0.0001 and ns (not significant), n.d. (not detected).

3.83 μM). Most importantly, exchange of the mouse C-terminus by that of the human enzyme in combination with the substitution Leu170His, Ile172Glu (chimera H), displayed a humanized phenotype, with an IC_{50} value of 561 ± 85 nM. Similar results were found for posaconazole (Fig. 7 and Table 2): the IC_{50} for chimera B and F were about two and three times lower than for the mouse enzyme, respectively. Substitution Leu170His,Ile172Glu in combination with the introduction of the human C-terminus (chimera H) further reduced the IC_{50}. Moreover, posaconazole was about three times less effective to inhibit chimera E and approximately 7-fold less potent to inhibit chimera A compared to the human enzyme.

4. Discussion

Recent clinical studies and case reports evidenced that the systemically used azole antifungals posaconazole and itraconazole can cause pseudohyperaldosteronism (reviewed in (Beck et al. 2020b)). Two distinct mechanisms were proposed, namely inhibition of the adrenal cortisol synthesis by CYP11B1, which seems to be the predominant mechanism for posaconazole (Barton et al. 2018; Boughton et al. 2018; Kuriakose et al. 2018; Beck et al. 2020a), and inhibition of cortisol inactivation by 11β-HSD2 in the kidney and colon, which seems to be the predominant mode-of-action for itraconazole (Hoffmann et al. 2018; Beck et al. 2020b). These adverse effects have only recently been recognized in patients, mainly in those reaching high serum drug levels, and they have remained unrecognized in preclinical investigations.

The present study revealed considerable species-specific differences in the inhibition of 11β-HSD2 by posaconazole, itraconazole and its main metabolite OHI. Regarding posaconazole, a very moderate difference of only 1.6-fold lower inhibitory activity was found against rat compared to human 11β-HSD2, in line with a previous estimation based on a comparison of human recombinant enzyme with whole rat kidney homogenate (Beck et al. 2017). Earlier toxicological studies in rats on the safety of posaconazole reported effects at high dose that were related to inhibition of steroid hormone synthesis; however, no information was provided on the underlying mechanism and typical symptoms of pseudohyperaldosteronism were not declared (European Medicines Agency 2019). Compared to posaconazole, itraconazole is a more potent inhibitor of human 11β-HSD2 (Beck et al. 2017). However, both itraconazole and its major metabolite OHI only moderately inhibited rat 11β-HSD2, in line with the previous preliminary assessment comparing human recombinant enzyme with whole rat kidney homogenate (Beck et al. 2017). This earlier experiment could not exclude a degradation of itraconazole and OHI by renal drug metabolizing enzymes, thus the present comparison of recombinant enzymes of the different species in an identical cellular background was needed. Interestingly, preclinical repeated-dose toxicity studies in rats assessing the safety of itraconazole did not detect any significant alterations of endocrine parameters (Van Cauteren et al. 1987). The lower sensitivity of rat compared to human 11β-HSD2 towards posaconazole and itraconazole may explain, at least in part, why pseudohyperaldosteronism as an adverse drug reaction has not been recognized in rodent preclinical studies. However, the difference in the inhibitory potency, especially of posaconazole, between rat and human 11β-HSD2 is very moderate and the reason why preclinical studies in rats did not reveal more pronounced effects on blood pressure and blood electrolytes are not fully understood. Further research should evaluate inter-individual as well as inter-species drug bioavailability. Regarding posaconazole, a recent study reported pseudohyperaldosteronism in only 20–25% of treated patients that also reached high serum concentrations (Nguyen et al. 2020). If rats exhibit a higher capacity to metabolize posaconazole and itraconazole than humans or if they have increased activity of efflux proteins, sufficiently high drug levels to inhibit 11β-HSD2 may not be reached in this species at the site of the target, *i.e.* kidney and adrenals. Both posaconazole and itraconazole also inhibit human CYP11B1 and CYP11B2; however, their inhibitory effects towards the rat enzymes remains to be determined. A lower inhibitory activity of these two azole antifungals towards rat CYP11B1 could also contribute to a lower risk for pseudohyperaldosteronism.

Blood pressure and blood electrolyte are usually measured in preclinical and clinical studies. If altered, pseudohyperaldosteronism could be detected by determination of serum renin and aldosterone. In case of low renin and aldosterone, further steroid analysis is indicated.

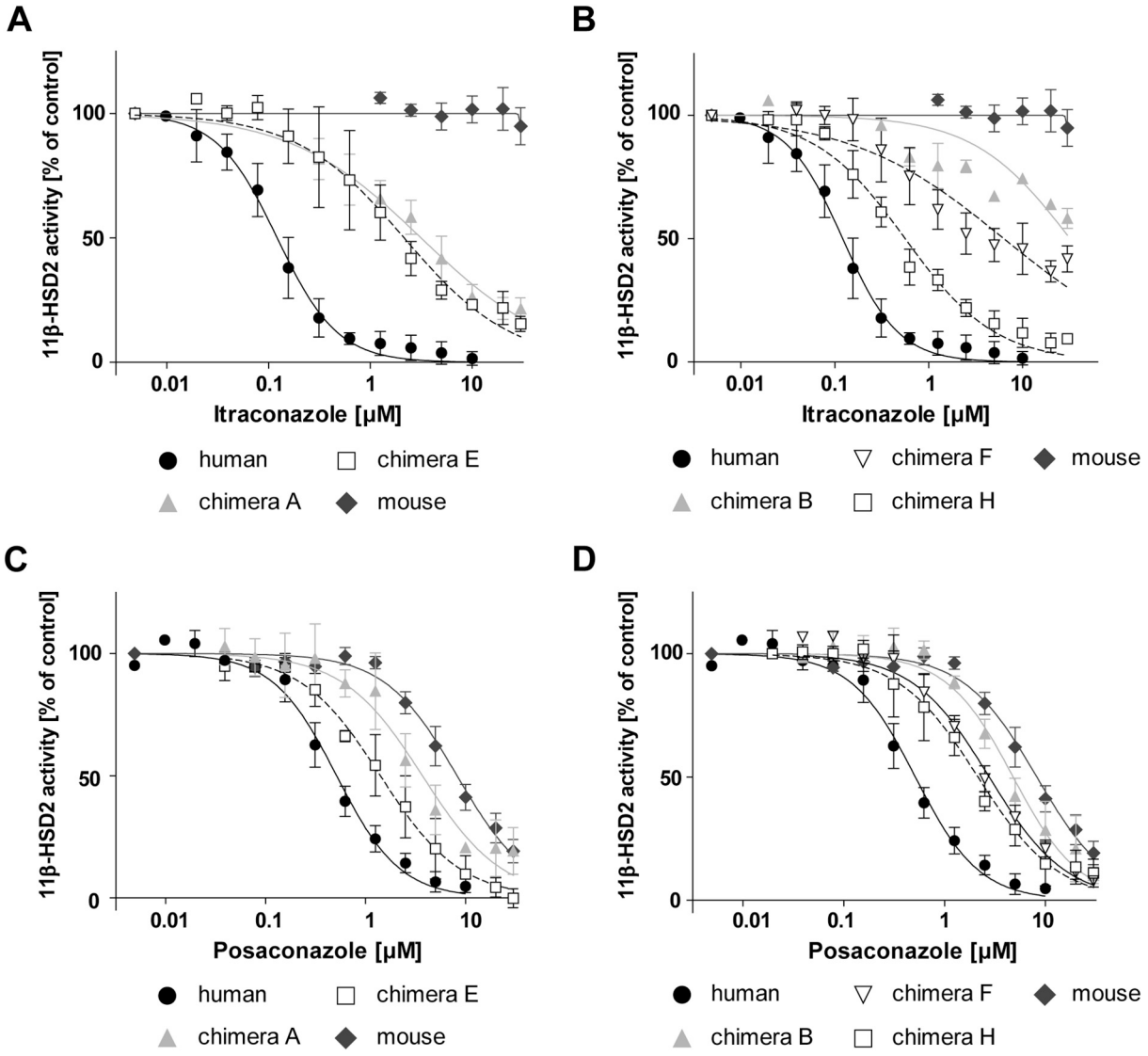

Fig. 7. Concentration-dependent inhibition of 11β-HSD2 variants by itraconazole and posaconazole. Lysates of HEK-293 cells expressing recombinant 11β-HSD2 of the indicated species or the respective chimera were incubated for 10 min (human, chimera B) or 20 min (mouse, chimera A, E, F, H) with 50 nM radiolabeled cortisol, 500 μM NAD^+ and increasing concentrations of itraconazole (A, B) and posaconazole (C, D). Substrate conversion was normalized to that of the vehicle control (0.6% DMSO for itraconazole and 0.3% DMSO for posaconazole). Data from three independent experiments are shown as mean ± SD.

Table 2
IC_{50} values for human and mouse 11β-HSD2 as well as for chimera A, B, E, F and H for itraconazole and posaconazole. 11β-HSD2 activity was determined in lysates of HEK-293 cells expressing the indicated 11β-HSD2 variant, measuring the conversion of cortisol to cortisone in presence of increasing concentrations of inhibitor. Inhibition curves were fitted and analyzed by non-linear regression. Data were normalized to vehicle control and represent mean ± SD of at three independent experiments. * % remaining activity at highest concentration of 30 μM.

		IC_{50} [μM]	
		Itraconazole	Posaconazole
Human		0.121 ± 0.030	0.512 ± 0.079
Mouse		(95%)*	8.212 ± 0.557
Chimera	A	3.55 ± 1.81	3.78 ± 1.58
	B	(58%)*	4.80 ± 1.66
	E	2.17 ± 1.66	1.40 ± 0.45
	F	6.34 ± 3.83	2.77 ± 0.38
	H	0.561 ± 0.085	2.30 ± 0.61

Increased serum and urinary ratios of active to inactive glucocorticoids are indicative of 11β-HSD2 inhibition and elevated 11-deoxycortisol and 11-deoxycorticosterone of CYP11B1 inhibition (Beck et al. 2020b).

An additional safety concern represents the disruption of the 11β-HSD2-mediated placental glucocorticoid barrier between mother and fetus. Inhibition of placental 11β-HSD2 can lead to elevated fetal exposure to cortisol, affecting fetal programming. An observational study in pregnant Finnish woman, assessing the effect of licorice intake (containing the potent 11β-HSD2 inhibitor GA) on pregnancy duration and health of the children, detected shorter gestation times, reduced birth weight, as well as an increased HPA axis activity and behavioral disturbances in the childhood (Strandberg et al. 2002; Räikkönen et al. 2009; Räikkönen et al. 2010). However, the use of azole antifungals is not indicated during pregnancy.

Importantly, the present study demonstrates that posaconazole and itraconazole (including OHI) are very weak inhibitors of mouse and zebrafish 11β-HSD2, with IC_{50} values above 7 μM. Whilst the mouse represents the most widely used species for mechanistic investigations, including transgene lines, the zebrafish is a frequently used model organism that gained increasing interest due to the low cost and the fact

that experiments with larvae are not considered as animal experiments (Planchart et al. 2016; Wrighton et al. 2019). Thus, mechanisms and possible consequences for human of 11β-HSD2 inhibition by these azole antifungals cannot be studied in these two species. Furthermore, as the concentrations of azole antifungals in the environment were reported to be in the picomolar range (Assress et al. 2019); the risk that itraconazole and posaconazole from wastewater affect fish health *via* 11β-HSD2 inhibition is negligible. Nevertheless, CYP11B1/2 that are also targets of posaconazole and itraconazole in human remain to be investigated as targets of these drugs in fish as well as in rodents (Beck et al. 2020a). This study emphasizes a cautious approach when trying to extrapolate findings from animal models to human. Species differences need to be taken into account when using animals as disease models or when investigating alternative 11β-HSD2 substrates, environmental inhibitors or potential therapeutic inhibitors.

To begin to understand the species-specific differences in the inhibition of 11β-HSD2 by the investigated azole antifungals, molecular modeling and chimeric enzymes with residue substitutions between human and mouse sequences were applied. As no 11β-HSD2 crystal structure is available to date, homology models were built for the human and mouse enzyme, based on human and guinea-pig 11β-HSD1 crystal structures, similar to previously reported models (Yamaguchi et al. 2011a; Yamaguchi et al. 2011b). In contrast to a recently reported model based on 17β-HSD1 structure (Yau et al. 2017), our attempts failed to find a suitable binding pose of cortisol allowing electron transfer to NAD^+ in 11β-HSD2 models derived from 17β-HSD1 structures. Furthermore, as shown in Fig. 8, superposition of 20 human homology models revealed the highly flexible C-terminal region for which no suitable structural prediction could be made due to the low similarity with any to-date crystallized protein. This emphasizes the uniqueness of the 11β-HSD2 C-terminal region compared to other short-chain dehydrogenase/reductase enzymes.

The roles of Trp276 and Arg279, suggested previously to be involved in the different response of human and mouse 11β-HSD2 to itraconazole and posaconazole (Beck et al. 2017), are difficult to predict by using homology models. Nevertheless, the influence of the non-conserved eight amino-acid long sequence located upstream of Trp276 was investigated by exchanging this cassette between human and mouse 11β-HSD2, followed by analysis of inhibitory effects. The observation that the exchange of this sequence did not alter the inhibition pattern for both chimeric enzymes compared to their wild type counterpart, suggests that a different positioning of Trp276 and Arg279 is not responsible for the observed species differences towards posaconazole and itraconazole. Alternatively, the substituted residues may not alter the different orientations of Trp276 and Arg279 in human and mouse 11β-HSD2.

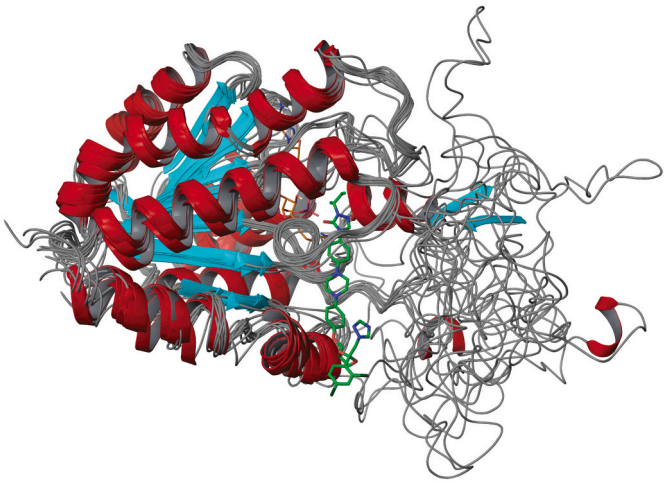

Fig. 8. Superposition of 20 human 11β-HSD2 homology models. Alpha helices are represented in red and beta sheets as arrows in turquoise. Itraconazole (green) and the cofactor NAD^+ (orange) were docked into the binding pocket. The high variability of the predicted C-terminal region is indicated by the unstructured grey lines. (For interpretation of the references to colour in this figure legend, the reader is referred to the web version of this article.)

Nevertheless, the C-terminal region had a partial effect on the species-specific inhibition of 11β-HSD2 by the studied azole antifungals. Itraconazole, its metabolite OHI and posaconazole have a prolonged rigid shape composed of consecutive rings, whereby the extended moiety of the molecule is oriented into the binding pocket to compete with the substrate and the rest of the molecule faces the C-terminal region of the enzyme (approximately 60% of the structure). In order to elucidate how such large rigid molecules can interact with residues in the C-terminal region, crystal structures with the cofactor and either cortisol or the respective inhibitor will be needed.

Besides the C-terminus, the active site loop comprising residues 168–180 was found to be responsible for part of the differences in the azole fungicide-mediated inhibition of 11β-HSD2 between human and mouse. The weak inhibition of mouse 11β-HSD2 by these compounds suggests that the lipophilic residues Leu170 and Ile172 at the analogous position of His170 and Glu172 in the human enzyme might cause steric hindrance, preventing the binding at this particular site. The homology model of mouse 11β-HSD2 can accommodate endogenous substrates like cortisol, but the bulky terminal groups of itraconazole and posaconazole are predicted to experience less favorable interactions compared to the human enzyme (Fig. 9, Video 3 and Video 4). In the human model, residue Glu172 is charged and expected to be oriented towards the solvent, leaving more room for bulky lipophilic ligands, while the amphiphilic character of histidine can be exploited. Substitution of Ile172 by glutamate in the mouse enzyme might induce conformational changes by reorientation of Glu172 to the solvent, thus increasing the size of the binding cavity, which consequently allows inhibition by the studied azole antifungals. Indeed, if the two residues 170 and 172 were mutated in the human enzyme to those present in mouse (chimera E), a substantial drop of inhibitory potency of itraconazole, OHI and posaconazole was seen. On the other hand, increased inhibition was observed, when the amino acids at position 170 and 172 in the mouse enzyme were changed to those in the human enzyme (chimera F).

Interestingly, a synergistic gain of inhibitory effect of itraconazole was observed when the mouse enzyme was mutated to bear the human C-terminal region and the Leu170His,Ile172Glu substitution. This chimeric enzyme represented the inhibitory pattern of human 11β-HSD2, indicating that both, residues in close proximity of the substrate and cofactor as well as residues in the C-terminal region, are involved in the potent inhibition by itraconazole. Interestingly, an interaction of the backbone of Asn171 with Arg279 located in the C-terminal region was proposed earlier to be important for the activity of the human enzyme (Yau et al. 2017). Asn171 was also proposed earlier to stabilize the binding of substrates (Fürstenberger et al. 2012) or of amino acids that interact with the pyrophosphate moiety of the cofactor (Arnold et al. 2003). Itraconazole and posaconazole might disturb such interactions and consequently inhibit human 11β-HSD2 activity. Whether mutation of the rat enzyme, or the zebrafish enzyme that is less conserved, at these positions leads to a humanized phenotype remains to be investigated.

In conclusion, the present study revealed significant species-specific differences in the inhibition of 11β-HSD2 by the azole antifungals itraconazole and posaconazole that have been missed in preclinical studies using rodents and that would also not be detected using zebrafish as an animal model. Predictions based on homology modeling and analysis of chimeric enzymes showed that substitution of Leu170,Ile172 in mouse 11β-HSD2 by the corresponding residues of the human enzyme, *i.e.* His170,Glu172, along with the exchange of the C-terminal region resulted in a gain of sensitivity towards inhibitory effect of these azole antifungals to resemble the pattern observed for the human enzyme. The derived structure-activity relationship information should facilitate follow-on studies to assess drugs with the potential to cause 11β-HSD2-

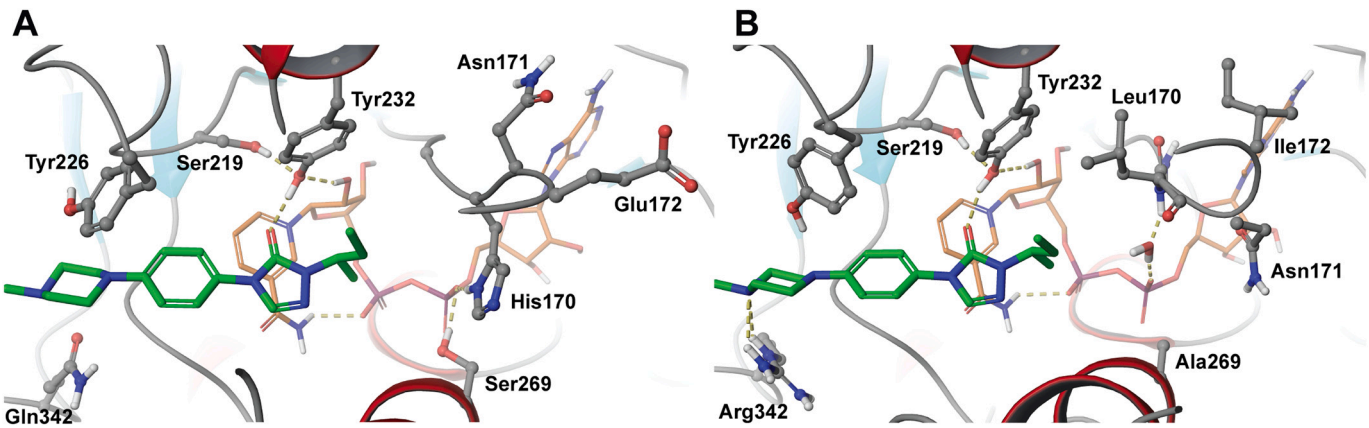

Fig. 9. Itraconazole (green) and NAD^+ (orange) docked into 11β-HSD2. A) human 11β-HSD2 and B) mouse 11β-HSD2 homology models. Hydrogen bond interactions (fulfilling directionality and distance criteria <2.8 Å) are depicted by yellow dashed lines. (For interpretation of the references to colour in this figure legend, the reader is referred to the web version of this article.)

dependent pseudohyperaldosteronism, and it should also be useful for the design of 11β-HSD2 inhibitors for specific therapeutic application and selection of adequate experimental animal models. In order to improve modeling-based predictions, mature artificial intelligence algorithms like AlphaFold capable of predicting the fold as well as crystal structures of 11β-HSD2 from different species in the presence of cofactor and substrate or inhibitor will be needed.

Supplementary data to this article can be found online at https://doi.org/10.1016/j.taap.2020.115387.

Declaration of Competing Interest

SGI, MZ, MS and AO declare no conflict of interest.

Acknowledgement

This work was supported by the Swiss Centre for Applied Human Toxicology (SCAHT).

References

Albiston, A.L., Obeyesekere, V.R., Smith, R.E., Krozowski, Z.S., 1994. Cloning and tissue distribution of the human 11 beta-hydroxysteroid dehydrogenase type 2 enzyme. Mol. Cell. Endocrinol. 105, R11–R17.

Arnold, P., Tam, S., Yan, L., Baker, M.E., Frey, F.J., Odermatt, A., 2003. Glutamate-115 renders specificity of human 11beta-hydroxysteroid dehydrogenase type 2 for the cofactor NAD+. Mol. Cell. Endocrinol. 201, 177–187.

Assress, H.A., Nyoni, H., Mamba, B.B., Msagati, T.A.M., 2019. Target quantification of azole antifungals and retrospective screening of other emerging pollutants in wastewater effluent using UHPLC -QTOF-MS. Environ. Pollut. 253, 655–666.

Barton, K., Davis, T.K., Marshall, B., Elward, A., White, N.H., 2018. Posaconazole-induced hypertension and hypokalemia due to inhibition of the 11β-hydroxylase enzyme. Clin. Kidney J. 11, 691–693.

Beck, K.R., Bächler, M., Vuorinen, A., Wagner, S., Akram, M., Griesser, U., Temml, V., Klusonova, P., Yamaguchi, H., Schuster, D., Odermatt, A., 2017. Inhibition of 11β-hydroxysteroid dehydrogenase 2 by the fungicides itraconazole and posaconazole. Biochem. Pharmacol. 130, 93–103.

Beck, K.R., Inderbinen, S.G., Kanagaratnam, S., Kratschmar, D.V., Jetten, A.M., Yamaguchi, H., Odermatt, A., 2019a. 11β-Hydroxysteroid dehydrogenases control access of 7β,27-dihydroxycholesterol to retinoid-related orphan receptor γ. J. Lipid Res. 60, 1535–1546.

Beck, K.R., Kanagaratnam, S., Kratschmar, D.V., Birk, J., Yamaguchi, H., Sailer, A.W., Seuwen, K., Odermatt, A., 2019b. Enzymatic interconversion of the oxysterols 7β,25-dihydroxycholesterol and 7-keto,25-hydroxycholesterol by 11β-hydroxysteroid dehydrogenase type 1 and 2. J. Steroid Biochem. Mol. Biol. 190, 19–28.

Beck, K.R., Telisman, L., van Koppen, C.J., Thompson 3rd, G.R., Odermatt, A., 2020a. Molecular mechanisms of posaconazole- and itraconazole-induced pseudohyperaldosteronism and assessment of other systemically used azole antifungals. J. Steroid Biochem. Mol. Biol. 199, 105605.

Beck, K.R., Thompson 3rd, G.R., Odermatt, A., 2020b. Drug-induced endocrine blood pressure elevation. Pharmacol. Res. 154, 104311.

Boughton, C., Taylor, D., Ghataore, L., Taylor, N., Whitelaw, B.C., 2018. Mineralocorticoid hypertension and hypokalaemia induced by posaconazole. Endocrinol Diabetes Metab Case Rep 2018.

Edwards, C.R., Stewart, P.M., Burt, D., Brett, L., McIntyre, M.A., Sutanto, W.S., de Kloet, E.R., Monder, C., 1988. Localisation of 11 beta-hydroxysteroid dehydrogenase–tissue specific protector of the mineralocorticoid receptor. Lancet 2, 986–989.

Edwards, C.R., Benediktsson, R., Lindsay, R.S., Seckl, J.R., 1993. Dysfunction of placental glucocorticoid barrier: link between fetal environment and adult hypertension? Lancet 341, 355–357.

European Medicines Agency, 2019. Noxafil, INN-posaconazole, Summary of Product Characteristics. https://www.ema.europa.eu/en/documents/product-information/noxafil-epar-product-information_en.pdf (accessed 4 August 2020).

Ferrari, P., 2010. The role of 11β-hydroxysteroid dehydrogenase type 2 in human hypertension. Biochim. Biophys. Acta 1802, 1178–1187.

Funder, J.W., Pearce, P.T., Smith, R., Smith, A.I., 1988. Mineralocorticoid action: target tissue specificity is enzyme, not receptor, mediated. Science 242, 583–585.

Fürstenberger, C., Vuorinen, A., Da Cunha, T., Kratschmar, D.V., Saugy, M., Schuster, D., Odermatt, A., 2012. The anabolic androgenic steroid fluoxymesterone inhibits 11β-hydroxysteroid dehydrogenase 2-dependent glucocorticoid inactivation. Toxicol. Sci. 126, 353–361.

Hoffmann, W.J., McHardy, I., Thompson 3rd, G.R., 2018. Itraconazole induced hypertension and hypokalemia: mechanistic evaluation. Mycoses 61, 337–339.

Inderbinen, S.G., Engeli, R.T., Rohrer, S.R., Di Renzo, E., Aengenheister, L., Buerki-Thurnherr, T., Odermatt, A., 2020. Tributyltin and triphenyltin induce 11β-hydroxysteroid dehydrogenase 2 expression and activity through activation of retinoid X receptor α. Toxicol. Lett. 322, 39–49.

Kuriakose, K., Nesbitt, W.J., Greene, M., Harris, B., 2018. Posaconazole-Induced Pseudohyperaldosteronism. Antimicrob. Agents Chemother. 62.

Lindsay, R.S., Lindsay, R.M., Waddell, B.J., Seckl, J.R., 1996. Prenatal glucocorticoid exposure leads to offspring hyperglycaemia in the rat: studies with the 11 beta-hydroxysteroid dehydrogenase inhibitor carbenoxolone. Diabetologia 39, 1299–1305.

Meyer, A., Strajhar, P., Murer, C., Da Cunha, T., Odermatt, A., 2012. Species-specific differences in the inhibition of human and zebrafish 11β-hydroxysteroid dehydrogenase 2 by thiram and organotins. Toxicology 301, 72–78.

Mune, T., Rogerson, F.M., Nikkilä, H., Agarwal, A.K., White, P.C., 1995. Human hypertension caused by mutations in the kidney isozyme of 11 beta-hydroxysteroid dehydrogenase. Nat. Genet. 10, 394–399.

Nguyen, M.H., Davis, M.R., Wittenberg, R., McHardy, I., Baddley, J.W., Young, B.Y., Odermatt, A., Thompson, G.R., 2020. Posaconazole serum drug levels associated with Pseudohyperaldosteronism. Clin. Infect. Dis. 70, 2593–2598.

Odermatt, A., 2004. Corticosteroid-dependent hypertension: environmental influences. Swiss Med. Wkly. 134, 4–13.

Odermatt, A., Kratschmar, D.V., 2012. Tissue-specific modulation of mineralocorticoid receptor function by 11β-hydroxysteroid dehydrogenases: an overview. Mol. Cell. Endocrinol. 350, 168–186.

Odermatt, A., Arnold, P., Stauffer, A., Frey, B.M., Frey, F.J., 1999. The N-terminal anchor sequences of 11beta-hydroxysteroid dehydrogenases determine their orientation in the endoplasmic reticulum membrane. J. Biol. Chem. 274, 28762–28770.

Planchart, A., Mattingly, C.J., Allen, D., Ceger, P., Casey, W., Hinton, D., Kanungo, J., Kullman, S.W., Tal, T., Bondesson, M., Burgess, S.M., Sullivan, C., Kim, C., Behl, M., Padilla, S., Reif, D.M., Tanguay, R.L., Hamm, J., 2016. Advancing toxicology research using in vivo high throughput toxicology with small fish models. Altex 33, 435–452.

Räikkönen, K., Pesonen, A.K., Heinonen, K., Lahti, J., Komsi, N., Eriksson, J.G., Seckl, J. R., Järvenpää, A.L., Strandberg, T.E., 2009. Maternal licorice consumption and detrimental cognitive and psychiatric outcomes in children. Am. J. Epidemiol. 170, 1137–1146.

Räikkönen, K., Seckl, J.R., Heinonen, K., Pyhälä, R., Feldt, K., Jones, A., Pesonen, A.K., Phillips, D.I., Lahti, J., Järvenpää, A.L., Eriksson, J.G., Matthews, K.A., Strandberg, T.E., Kajantie, E., 2010. Maternal prenatal licorice consumption alters

hypothalamic-pituitary-adrenocortical axis function in children. Psychoneuroendocrinology 35, 1587–1593.
Raleigh, D.R., Sever, N., Choksi, P.K., Sigg, M.A., Hines, K.M., Thompson, B.M., Elnatan, D., Jaishankar, P., Bisignano, P., Garcia-Gonzalo, F.R., Krup, A.L., Eberl, M., Byrne, E.F.X., Siebold, C., Wong, S.Y., Renslo, A.R., Grabe, M., McDonald, J.G., Xu, L., Beachy, P.A., Reiter, J.F., 2018. Cilia-associated Oxysterols activate smoothened. Mol. Cell 72, 316–327.
Sastry, G.M., Adzhigirey, M., Day, T., Annabhimoju, R., Sherman, W., 2013. Protein and ligand preparation: parameters, protocols, and influence on virtual screening enrichments. J. Comput. Aided Mol. Des. 27, 221–234.
Seckl, J.R., Cleasby, M., Nyirenda, M.J., 2000. Glucocorticoids, 11beta-hydroxysteroid dehydrogenase, and fetal programming. Kidney Int. 57, 1412–1417.
Stewart, P.M., Rogerson, F.M., Mason, J.I., 1995. Type 2 11 beta-hydroxysteroid dehydrogenase messenger ribonucleic acid and activity in human placenta and fetal membranes: its relationship to birth weight and putative role in fetal adrenal steroidogenesis. J. Clin. Endocrinol. Metab. 80, 885–890.
Strandberg, T.E., Andersson, S., Järvenpää, A.L., McKeigue, P.M., 2002. Preterm birth and licorice consumption during pregnancy. Am. J. Epidemiol. 156, 803–805.
Thompson 3rd, G.R., Chang, D., Wittenberg, R.R., McHardy, I., Semrad, A., 2017. In Vivo 11β-Hydroxysteroid Dehydrogenase Inhibition in Posaconazole-Induced Hypertension and Hypokalemia. Antimicrob Agents Chemother 61.
Thompson 3rd, G.R., Beck, K.R., Patt, M., Kratschmar, D.V., Odermatt, A., 2019. Posaconazole-Induced Hypertension Due to Inhibition of 11β-Hydroxylase and 11β-Hydroxysteroid Dehydrogenase 2. J Endocr Soc 3, 1361–1366.
Van Cauteren, H., Heykants, J., De Coster, R., Cauwenbergh, G., 1987. Itraconazole: pharmacologic studies in animals and humans. Rev. Infect. Dis. 9 (Suppl. 1), S43–S46.
Voisin, M., de Medina, P., Mallinger, A., Dalenc, F., Huc-Claustre, E., Leignadier, J., Serhan, N., Soules, R., Ségala, G., Mougel, A., Noguer, E., Mhamdi, L., Bacquié, E., Iuliano, L., Zerbinati, C., Lacroix-Triki, M., Chaltiel, L., Filleron, T., Cavaillès, V., Al Saati, T., Rochaix, P., Duprez-Paumier, R., Franchet, C., Ligat, L., Lopez, F., Record, M., Poirot, M., Silvente-Poirot, S., 2017. Identification of a tumor-promoter cholesterol metabolite in human breast cancers acting through the glucocorticoid receptor. Proc. Natl. Acad. Sci. U. S. A. 114, E9346–E9355.
Wassermann, T., Reimer, E.K., McKinnon, M., Stock, W., 2018. Refractory Hypokalemia from syndrome of apparent mineralocorticoid excess on low-dose Posaconazole. Antimicrob. Agents Chemother. 62.
White, P.C., Mune, T., Agarwal, A.K., 1997. 11 beta-Hydroxysteroid dehydrogenase and the syndrome of apparent mineralocorticoid excess. Endocr. Rev. 18, 135–156.
Wilson, R.C., Harbison, M.D., Krozowski, Z.S., Funder, J.W., Shackleton, C.H., Hanauske-Abel, H.M., Wei, J.Q., Hertecant, J., Moran, A., Neiberger, R.E., et al., 1995. Several homozygous mutations in the gene for 11 beta-hydroxysteroid dehydrogenase type 2 in patients with apparent mineralocorticoid excess. J. Clin. Endocrinol. Metab. 80, 3145–3150.
Wrighton, P.J., Oderberg, I.M., Goessling, W., 2019. There is something fishy about liver Cancer: Zebrafish models of hepatocellular carcinoma. Cell Mol Gastroenterol Hepatol 8, 347–363.
Yamaguchi, H., Akitaya, T., Kidachi, Y., Kamiie, K., Noshita, T., Umetsu, H., Ryoyama, K., 2011a. Mouse 11β-hydroxysteroid dehydrogenase type 2 for human application: homology modeling, structural analysis and ligand-receptor interaction. Cancer Inform 10, 287–295.
Yamaguchi, H., Akitaya, T., Yu, T., Kidachi, Y., Kamiie, K., Noshita, T., Umetsu, H., Ryoyama, K., 2011b. Homology modeling and structural analysis of 11β-hydroxysteroid dehydrogenase type 2. Eur. J. Med. Chem. 46, 1325–1330.
Yau, M., Haider, S., Khattab, A., Ling, C., Mathew, M., Zaidi, S., Bloch, M., Patel, M., Ewert, S., Abdullah, W., Toygar, A., Mudryi, V., Al Badi, M., Alzubdi, M., Wilson, R. C., Al Azkawi, H.S., Ozdemir, H.N., Abu-Amer, W., Hertecant, J., Razzaghy-Azar, M., Funder, J.W., Al Senani, A., Sun, L., Kim, S.M., Yuen, T., Zaidi, M., New, M.I., 2017. Clinical, genetic, and structural basis of apparent mineralocorticoid excess due to 11β-hydroxysteroid dehydrogenase type 2 deficiency. Proc. Natl. Acad. Sci. U. S. A. 114, E11248–E11256.